Modelling the impact of deterioration on the long-term performance of Dublin Tunnel

Chao Wang[1,2], Zhipeng Xiao[1], Miles Friedman[3] and Zili Li[1,2*]

[1]Civil, Structural and Environmental Engineering, University College Cork, Cork, Ireland

[2]Irish Centre for Research in Applied Geosciences, University College Dublin, Dublin, Ireland

[3]Transport Infrastructure Ireland, Parkgate Business Centre, Parkgate Street, Dublin 8, Ireland

[*]Corresponding author: zili.li@ucc.ie

ABSTRACT: The influence of tunnel deteriorations like hydraulic and mechanical deterioration on its long-term performance has received extensive attention recently. Most studies considered deteriorations by manually varying the magnitude of parameters like permeability and stiffness, often neglecting their time-dependent variation process (individual/coupled). This paper addresses this gap by investigating the impact of time-dependent hydraulic and mechanical deteriorations on the long-term behaviour of the aging Dublin Port Tunnel (DPT). Relevant geotechnical and mechanical properties of ground layers and concrete lining were firstly characterised and determined. A modified analytical relative ground-lining permeability (*RP*) model and calculated deteriorated lining permeability for DPT were presented, with steps and procedures generalised. The deteriorated permeability of DPT was incorporated into the hydraulic deterioration model thereafter, together with tunnel mechanical deterioration, offering a more holistic and realistic prediction of DPT's deterioration-induced long-term performance than previously available. Numerical results, compared against field measurements, showed that (1) assuming constant tunnel permeability during its lifetime fails to accurately capture time-dependent liner deformation, and hydraulic deterioration has been identified as the dominant factor inducing an approaching squatting deformation mode, which can be attributed to twin tunnel interaction effect; (2) continuous mechanical deterioration leads to a linear growth in both vertical and horizontal convergence over time, with vertical convergence being more pronounced, indicating a squatting contraction deformation mode that could be associated with reduced ability to support ground pressure and external loads; (3) the comparison quantitatively evaluates the impact of individual and coupled hydro-mechanical deterioration on DPT's long-term behaviour and the agreement between field data and numerical results confirms that coupled lining deterioration is the root cause behind the monitored lining deformation.

KEYWORDS: relative ground-lining permeability; hydraulic and mechanical deterioration; coupled deterioration; tunnel long-term performance; finite element modelling

1. INTRODUCTION

Tunnel structures experience different levels of deterioration over their lifespan as they interact with surrounding environment. Deteriorations, like water leakage and concrete cracking, could disrupt tunnel operations, compromise tunnel serviceability, or even threaten its long-term integrity and safety, if not proper controlled and managed (Wang et al. 2023). Dublin Port Tunnel (DPT, also Dublin Tunnel), the biggest Irish urban road tunnel, has exhibited local deteriorations since its opening in 2006. Onsite inspection and maintenance records identified water leakage, concrete cracking and spalling as the three greatest long-term concerns for tunnel operation (Wang et al. 2023).

Lining deteriorations can typically be categorised as hydraulic and mechanical deterioration. Liner hydraulic deterioration, the most common type of deterioration, usually manifests as blockages in tunnel drainage systems (Kim et al. 2020) and increasing water leakage (Li et al. 2020). Blockages can result from fine particle accumulation in drainage paths, reducing tunnel discharge capacity and increasing pore water pressure (Shin et al. 2005). However, tunnel leakage is related to the expansion/propagation of concrete cracks and/or construction joints, expanding water flow paths and increasing water inflow (Shin et al. 2005). Both deteriorations alter lining's hydraulic status and permeability, affecting its mechanical and deformational behaviour (Kim et al. 2020; Li et al. 2020; Shin et al. 2012; Yoo 2016). However, the current paper only focuses on the influence of the latter. Regarding cracking/joint-related hydraulic deterioration, Picandet et al. (2009) found the overall permeability of deteriorated concrete rises as existing cracks widen (i.e., crack width) and new cracks form (i.e., crack density). Similarly, Yi et al. (2011) observed that a progressive increase in lining crack width and density facilitates the interconnection of water flow paths, leading to higher lining permeability. Despite extensive research efforts on tunnel hydraulic deterioration, many studies still overlook the effects of deteriorated lining permeability and time-dependent deterioration.

Laver et al. (2013) performed permeability experiments on intact but degraded grout samples from London Underground tunnels to derive lining's deteriorated permeability, but the intrusive grout/lining sampling is practically unacceptable to asset owners. Bagnoli et al. (2015) estimated the current tunnel permeability using inverse-analysis to match water flow-conductivity data from numerical simulations

with varying hydraulic conductivity. Li et al. (2020) derived lining permeability for segmental tunnels by considering joint opening between lining rings, on the basis of a jointed rock permeability model. To avoid direct permeability calculations, Wongsaroj et al. (2013) proposed using relative soil-lining permeability (*RP*) to evaluate the hydraulic conditions of tunnel excavated in London Clay, by equating water flow through London Clay and tunnel liner on the basis of assuming 1D water flow during post-excavation consolidation. Laver et al. (2017) later refined the proposed 1D *RP* model by assuming a 2D radial water flow mode around tunnel linings.

Apart from hydraulic deterioration, liner mechanical deterioration also significantly affects tunnel bearing capacity and thus long-term deformation due to various negative influences, such as physical attacks (e.g., frost action), chemical influences (e.g., ions penetration) and biological processes (Idris et al. 2009; Usman and Galler 2013). Usman and Galler (2013) modelled the impact of lining mechanical deterioration through reducing the Young's modulus, cohesion and friction angle of shotcrete lining. Similarly, Závacký et al. (2018) simulated concrete deterioration and reinforcement corrosion through reducing liner stiffness and thickness. Showkati et al. (2021) found tunnel support system mechanical deterioration transfers load to the final lining, and enables the formation of a plastic zone surrounding the tunnel and an increase in lining axial thrust and bending moment. Xu et al. (2021) examined the impact of freeze-thaw cycles on tunnel performance and found increased cycles decrease tunnel bearing capacity. Sandrone and Labiouse (2010) concluded rock mass deterioration impacts tunnel performance in the medium term, while liner deterioration is more significant in the long run. Han and Jeong (2014) observed liner mechanical deterioration induces an increasing ground and tunnel settlement, and greater lining internal forces and increasing tunnel convergence over time.

Reviewing the influences of deterioration above reveals several aspects that were largely neglected and can be improved: (1) realistic estimates of deteriorated lining permeability and tunnel deterioration assessment, (2) modelling time-dependent lining deterioration within tunnel's operational lifespan, and (3) the lack of field monitoring data to verify conclusions from analytical/numerical studies. To address these gaps and limitations, this paper develops a 3D coupled hydraulic-mechanical numerical model of a critical vehicle cross passage (VCP) section of Dublin Port Tunnel to study the individual and coupled

effects of tunnel hydraulic and mechanical deteriorations on DPT's long-term performance. Specifically, the hydraulic and mechanical deterioration of the selected DPT section is modelled by time-dependent variation in lining permeability and stiffness, respectively, and details regarding the modelling of both deteriorations are presented in section 4.2.

The current paper focuses on modelling how hydraulic, mechanical and coupled hydro-mechanical deterioration affect the long-term performance of a selected section of Dublin Tunnel. Section 2 details the characterisation and identification of mechanical, hydraulic and geotechnical parameters of ground and lining. Section 3 presents general steps and procedures to derive the modified relative permeability model, to calculate the deteriorated liner permeability and to assess DPT's hydraulic deterioration status based on groundwater inflow data in a pioneering attempt. Section 4 presents the modelling and results of hydraulic, mechanical and coupled hydro-mechanical deterioration effects and compares numerical results against field data to investigate the main cause of the observed long-term tunnel deformation.

2. DUBLIN PORT TUNNEL PROFILE

2.1 DPT geotechnical profile

The construction of Dublin Port Tunnel comprises three distinct sections, namely, a northern cut and cover section, an in-between bored tunnel section, and a southern cut and cover section, and encounters various geological strata at different depths. The VCP 16 section, the focus of this study, is situated at the lowest point of the tunnel longitudinal alignment, as illustrated in Figure 1(*a*). This section is of special concern because of the observed critical tunnel deterioration such as water leakage, lining cracks and concrete spalling. With reference to the face-logs collected during tunnel excavation, the nearest available borehole logs and previous studies on the geology around DPT (Kovacevic et al. 2008; Long and Menkiti 2007a; Skipper et al. 2005), a simplified vertical ground profile around VCP 16 section is given in Figure 1(*b*). The VCP 16 tunnel section is approximately 19.5m below ground surface in argillaceous limestone (G3), with overlying soil layers of sandy clayey gravel (G1) and sandy gravelly clay (G2) which can both be generally categorised as "Dublin Boulder Clay" according to previous investigations (Cabarkapa et al. 2003; Kovacevic et al. 2008; Lawler et al. 2010). This dense, stiff and low-permeability soil covers a significant portion of Dublin city, inclusive of the DPT area, as the main

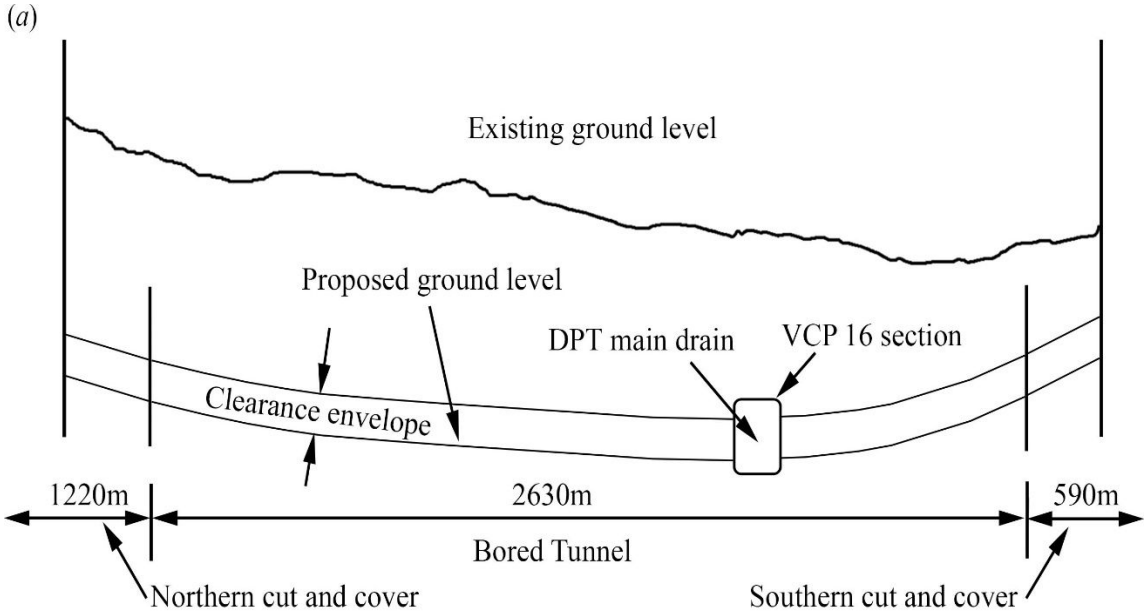

(*a*) Alignment of Dublin Port Tunnel

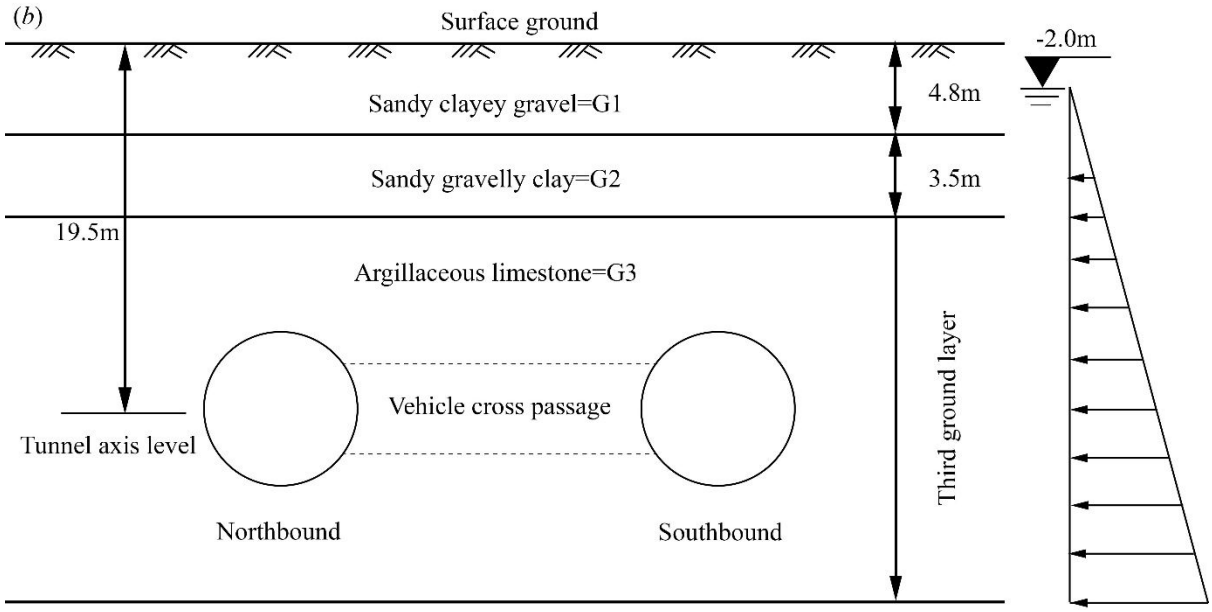

(*b*) Ground profile around VCP 16 section

Figure 1. Dublin Port Tunnel alignment and ground profile (Wang et al. 2023)

surface glacial deposit. This soil was originally classified as cohesive. However, recent research efforts by Trinity College Dublin and University College Dublin, based on comprehensive laboratory tests, have proposed that it is more accurate to describe it as a frictional material (Long and Menkiti 2007b). Most studies assumed the effective cohesion of this type of soil to be zero and effective friction angle

within 30°-35°, with the at-rest earth pressure coefficient within 1.0-1.5 and permeability coefficient between 10^{-08} m/s and 10^{-11}m/s (Cabarkapa et al. 2003; Lehane and Simpson 2000; Long and Menkiti 2007b). However, due to the extensive existence of sands and gravels in G1 and G2 for the VCP 16 section, the in-situ test results showed a higher permeability within 10^{-06} m/s and 10^{-08}m/s. The initial groundwater conditions were hydrostatic with the water table at approximately 2.0m below ground surface. The material properties of the two soil layers and limestone layer are summarised in Table 1.

Although the majority of material properties have been obtained and identified, the two shear strength parameters, cohesion (c) and internal friction angle (φ), for the rock unit limestone remains to be determined. Sivakugan et al. (2014) proposed using Mohr-Coulomb (M-C) failure criterion to derive the rock shear strength parameters by adopting Brazilian tensile strength test results (BTS test) and uniaxial compressive strength test results (UCS test), with the calculations of the two shear strength parameters shown in the following two equations (1) and (2).

$$\varphi = \sin^{-1}((\sigma_c - 4\sigma_t)/(\sigma_c - 2\sigma_t)) \quad (1)$$

$$c = 0.5\sigma_c\sigma_t/\sqrt{\sigma_t(\sigma_c - 3\sigma_t)} \quad (2)$$

Where σ_c and σ_t are the UCS and BTS of rock, MPa, respectively. The statistical values of the estimated shear strength parameters can then be calculated with the substitution of UCS and BTS of limestone. The material properties of both ground layers and lining concrete (LC) are then updated in Table 1.

Table 1. Material properties of ground units and lining concrete

Property	G1	G2	G3	LC
Dry density ρ_d (g/cm^3)	2.0	2.0	2.6	2.5
Elastic modulus E	60.0 MPa	100.0 MPa	3.82 GPa	30.0 GPa
Poisson's ratio v	0.30	0.30	0.15	0.20
Material cohesion c	0.0	0.0	30.0MPa	/
Friction angle φ (°)	30.0	35.0	48.0	/
Initial permeability k_{ini} (m/s)	6.4×10^{-08}	4.8×10^{-06}	6.1×10^{-08}	2.0×10^{-13}
BTS (MPa)	/	/	16.0 MPa	/
UCS (MPa)	/	/	156.0 MPa	/

2.2 DPT hydraulic profile

As the biggest urban road tunnel in Ireland, DPT is outfitted with a comprehensive waterproofing and drainage system. The structural components of the 2.63km-long bored section consist of annular grout, segmental lining and in-situ secondary lining, with waterproofing membranes deployed between these structural layers and positive drains implemented to facilitate groundwater discharge, as depicted in Figure 2. Groundwater drainage for this section is directed towards the main drainage sump located under the invert of each bore, as demonstrated in Figure 1(*a*). Designed to remain watertight during its operational lifespan, the twin-bore tunnel originally had a lining segment initial permeability of 2.0×10^{-13}m/s. Upon its opening in 2006, water ingress was detected at various points, including VCP 16, leading to repairs involving local replacements of waterproofing membranes and concrete. Further inspections and maintenance have shown that the tunnel's deteriorations, such as lining cracks and water infiltration, have progressively increased over time, as indicated in Figure 3. However, the tunnel liner permeability and rate of deterioration for Dublin Port Tunnel after a decade plus operation are yet to be determined. In the following section, based on a modified analytical model for relative ground-lining permeability proposed in Wang et al. (2022), the general steps and processes for such derivation and the calculation of the deteriorated lining permeability using field water inflow data monitored over the previous nine years were firstly presented, followed by generalising the steps and procedures for assessing lining hydraulic deterioration status after more than a decade's operation.

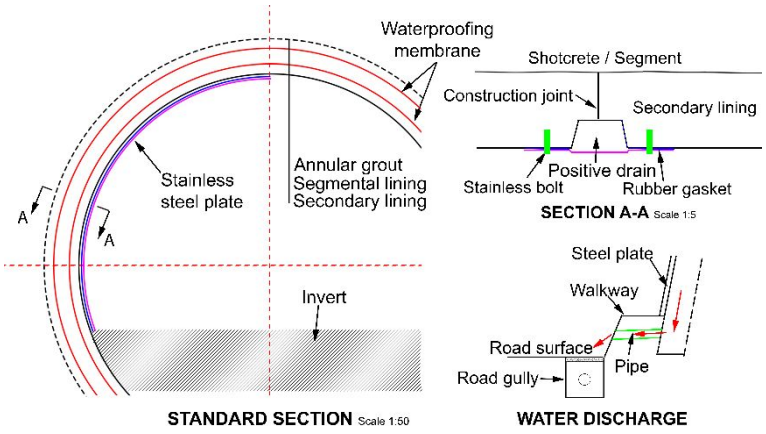

Figure 2. DPT typical waterproofing and drainage system

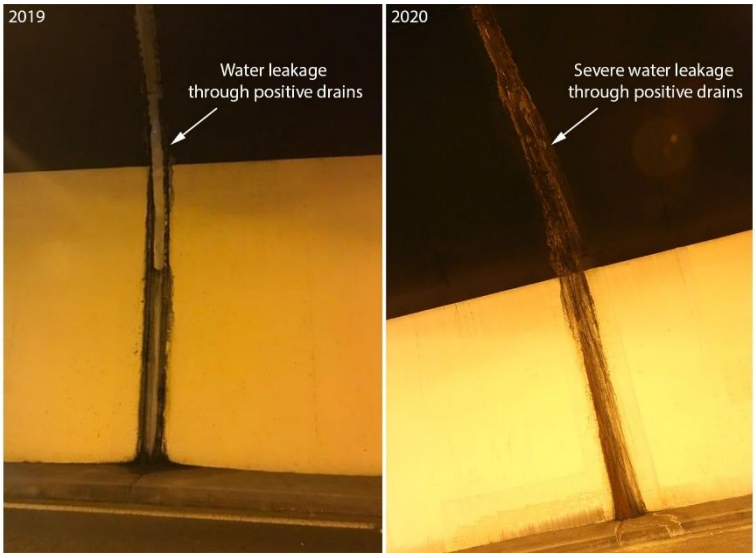

Figure 3. Progressive tunnel lining deteriorations at VCP 16 section

3. GROUND-LINING RELATIVE PERMEABILITY

3.1 Previous *RP* definitions

To assess the behaviour of a London Clay-embedded tunnel in the long term, two relative permeability definitions were proposed in two respective studies (Laver et al. 2017; Wongsaroj et al. 2013). Both studies assumed (1) a constant water table in the sandy soil layer above the London Clay layer, (2) an equal groundwater flow through London Clay layer and tunnel lining, and (3) groundwater only flows through London Clay layer (Laver et al. 2017; Wongsaroj et al. 2013). As the first attempt, Wongsaroj et al. (2013) obtained the relative ground-lining permeability *RP* by employing Darcy's law for a hypothetical 1D consolidation flow scenario in London Clay and by assuming 1D flow downward only from tunnel crown. Through equating the water inflow through London Clay layer and tunnel lining, the relative ground-lining permeability model was proposed, as can be seen in Figure 4. Laver et al. (2017) later improved Wongsaroj et al. (2013)'s model by adopting a more realistic water inflow pattern into the tunnel, where the hydraulic field around the tunnel was considered as a radial flow model, as demonstrated in Figure 4.

Assumptions: (1) constant water table;(2) Equal water flow through ground and lining based on hydraulic continuity

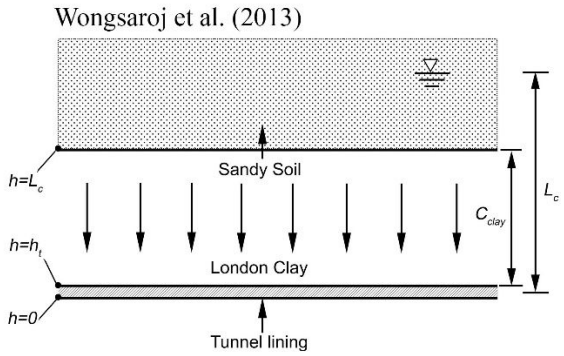

One-dimensional flow model (Wongsaroj et al., 2013)

Groundwater flows through London Clay following Darcy's law $k_g(L_c-h_t)/C_{clay}$

Equals =

Groundwater flows through tunnel lining in following Darcy's law $k_t h_t/t_t$

$$RP=C_{clay}k_t/k_g t_t \text{ where } h_t/L_c=1/(1+RP)$$

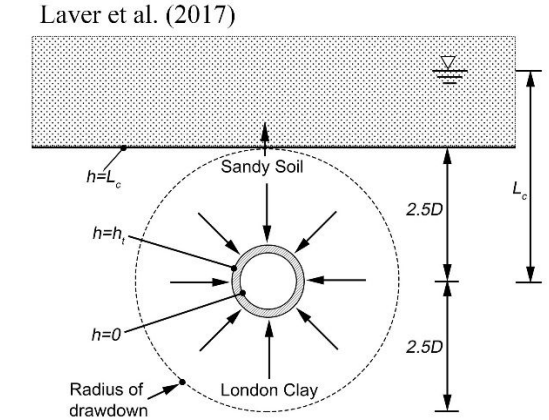

Two-dimensional radial flow model (Laver et al., 2017)

Water flows through London Clay following 2D radial pattern $q_g=2\pi r k_g dh/dr$

Equals =

Water flows through unit lining length following Darcy's law $q_t=\pi D k_t h_t/t_t$

$$RP=Dk_t/(2k_g t_t)\times\ln(2C_{clay}/D+1)$$

RP - relative permeability C_{clay} - Depth of London Clay ground layer k_g - Ground permeability k_t - Lining permeability

L_c - Depth between water table and tunnel lining h_t - Hydraulic head at lining extrados t_t - Lining thickness D - Tunnel external diameter

Figure 4. *RP* definitions by previous studies (Laver et al. 2017; Wongsaroj et al. 2013)

3.2 *RP* definition for Dublin Port Tunnel (Wang et al. 2022)

Earlier research by Wongsaroj et al. (2013) and Laver et al. (2017) concentrated on tunnels constructed in London Clay beneath sandy soils. Both studies presumed that, over the long term, soil consolidation flow happens exclusively within the less permeable London Clay layer. However, this assumption does not apply to the geological conditions around the section of interest in this study, as shown in Figure 1(*b*), where the tunnel section is located in argillaceous limestone, with two overlying clayey soil layers. A quarter model of the VCP 16 section, illustrated in Figure 5 and Figure 9, reveals that the layby tunnel does not have a circular shape, unlike the circular tunnels described in the two preceding studies. However, in the context of the entire 2.63 km-long bored tunnel section, the combined length of the two layby sections amounts to just a minor 80 meters. To develop an analytical solution, certain assumptions about the tunnel section's characteristics and conditions are made below: (1) the anisotropy of the tunnel lining's permeability is disregarded; (2) the water table, positioned 2.0 meters below the ground surface, is considered stable over time; (3) groundwater is assumed to flow towards the tunnel in a radial pattern; and (4) the shape of this layby-VCP section is treated as a circular tunnel, matching the external diameter of the bored tunnel at 11.22 meters (Wang et al. 2022).

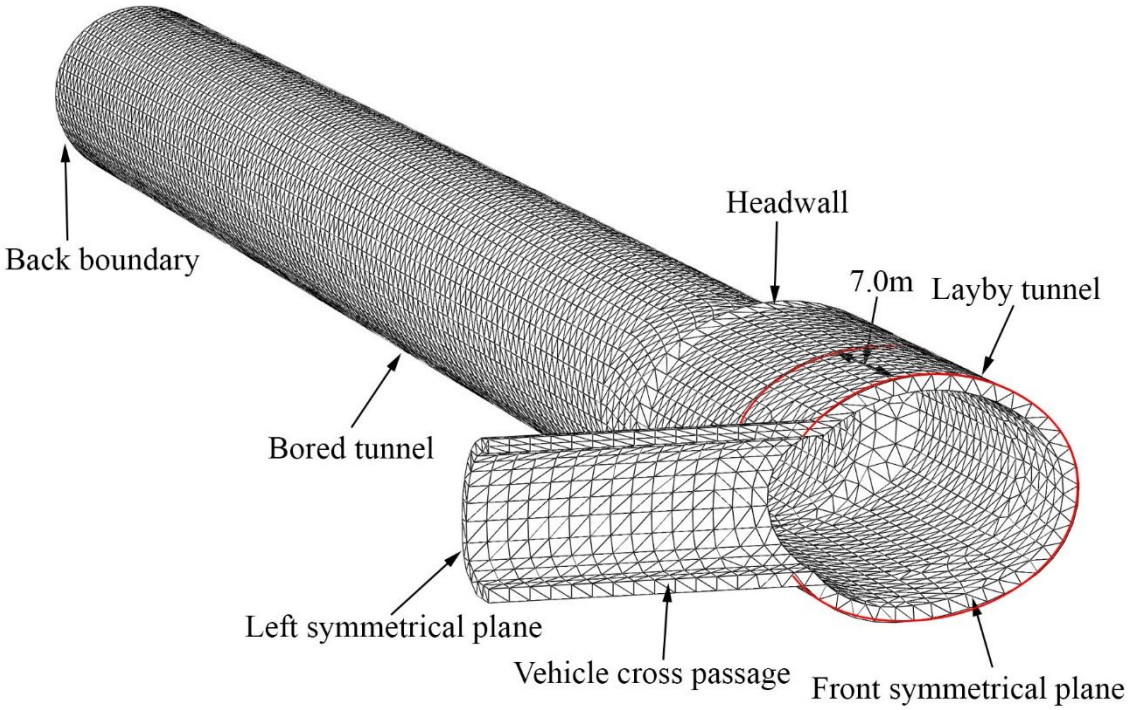

Figure 5. Components of VCP 16 section (adapted from Wang et al. 2022)

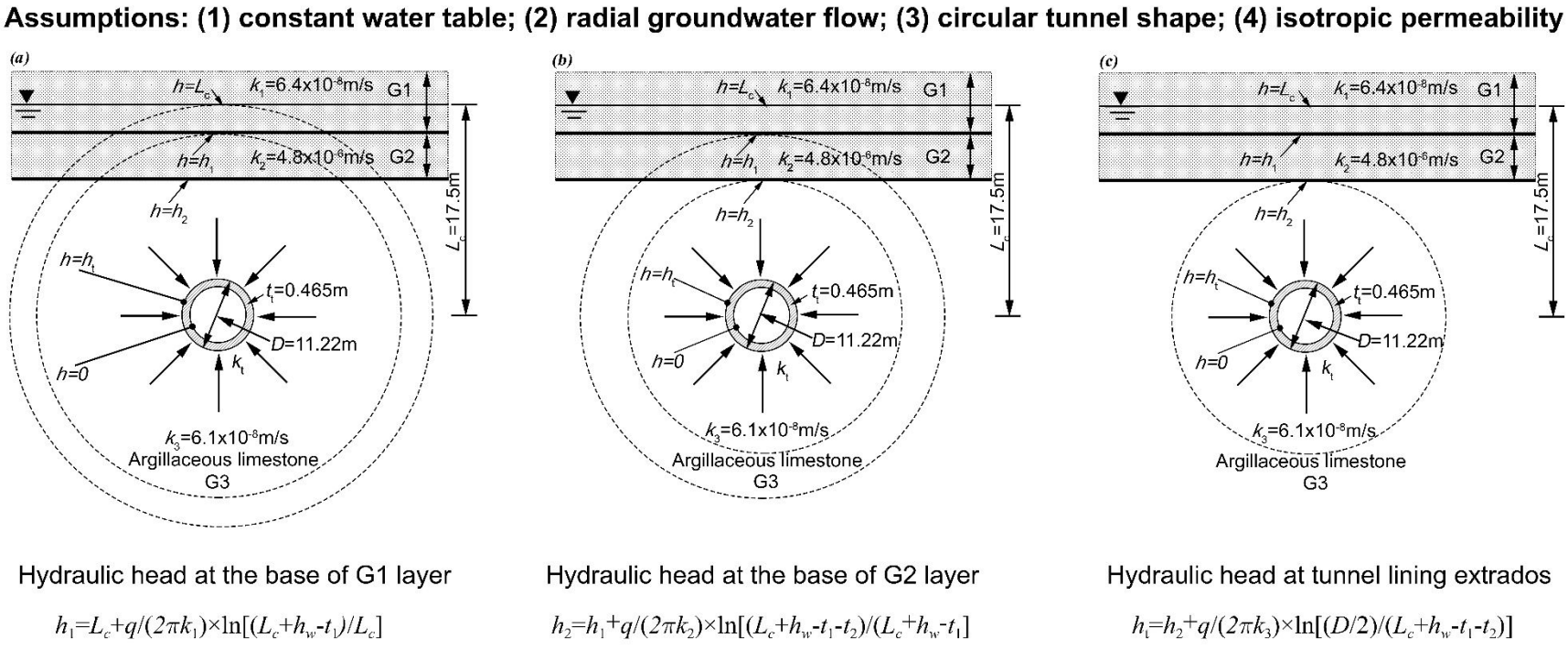

Figure 6. Mathematical model for Dublin Port Tunnel *RP* derivation (Wang et al. 2022)

Based on the mathematical model proposed in the previous two studies for deriving the relative ground-lining permeability, Figure 6 shows the mathematical model for deriving the *RP* for Dublin Port Tunnel. As the derivation has been covered in a prior study by the authors Wang et al. (2022), this section only presents a summary of the derivation. The detailed derivation steps can be found in Wang et al. (2022). Based on *RP* derivation in Laver et al. (2017), Figure 7 gives a flowchart for deriving the *RP* for DPT. Generally, it was divided into three main steps: (1) firstly, appropriate assumptions about *RP* derivation for DPT need to be made; (2) secondly, the model is derived on the basis of equating groundwater flow through ground layers and tunnel lining, subject to certain relevant boundary conditions; (3) lastly, the derived *RP* model needs to be modified following the equivalent permeability for all three ground layers.

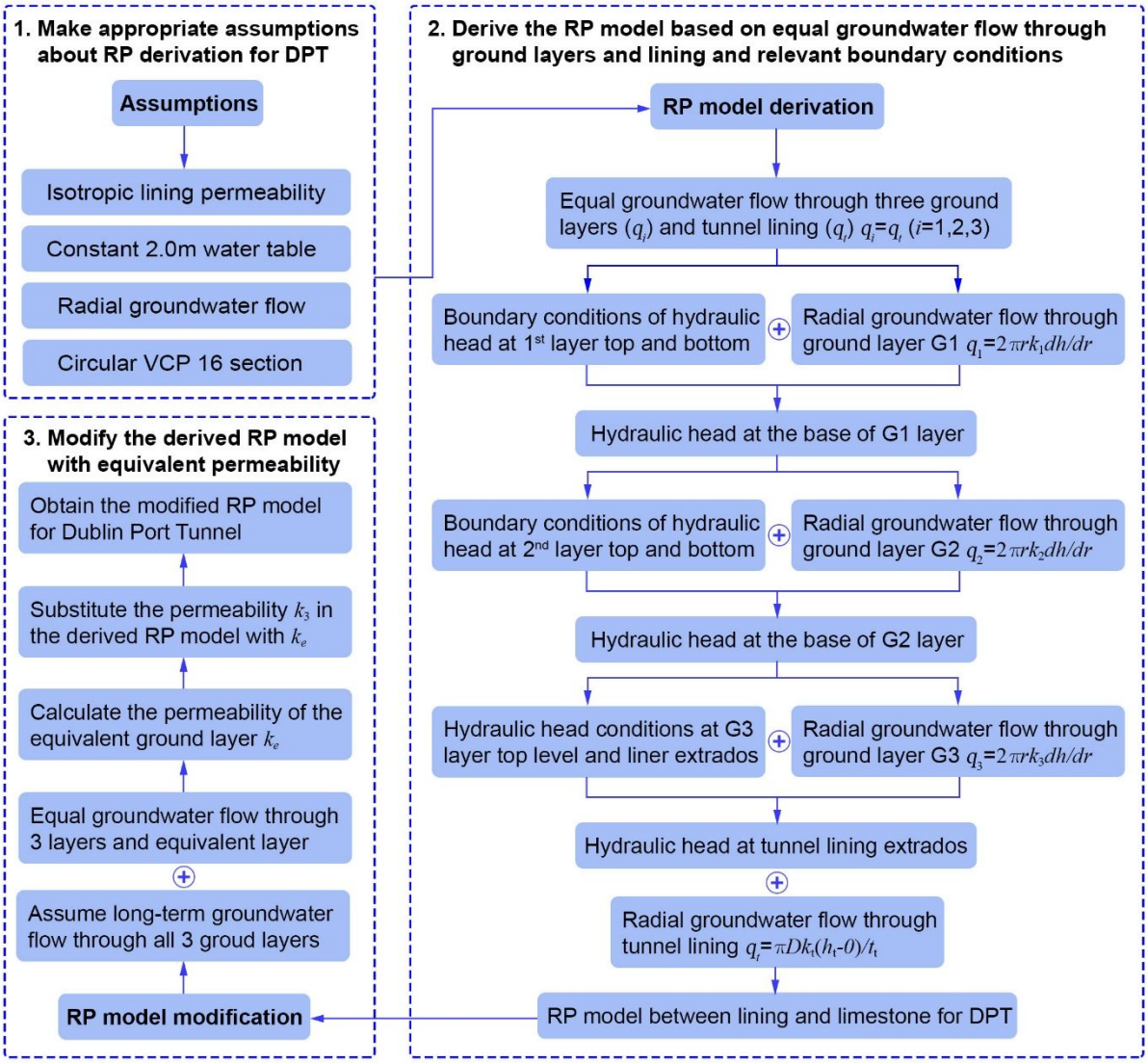

Figure 7. Flowchart for the *RP* derivation for DPT

Following the first two main steps, the relative permeability model between lining and argillaceous limestone for DPT can be derived as follows (Wang et al. 2022):

$$h_t/h_2 = 1/(1 + RP) \tag{3}$$

$$RP = Dk_t/(2t_t k_3) \times \ln[2(L_c + h_w - t_1 - t_2)/D] \tag{4}$$

As outlined earlier, the relative permeability *RP*, as proposed in Wongsaroj et al. (2013) and Laver et al. (2017), was determined on the basis of assuming that long-term water flow occurs solely in the less permeable London Clay, excluding the highly permeable sandy soil layer. However, this assumption does not hold for DPT, where the permeability of the two layers above the argillaceous limestone cannot be ignored, as the permeability of these three layers is roughly equal (Wang et al. 2022). Therefore, in equation (4), the ground permeability k_3 should be substituted with the equivalent permeability k_e of the three layers (Wang et al. 2022). The detailed derivation steps for k_e can be found in Wang et al. (2022). Therefore, the modified relative permeability model for DPT can then be updated as (Wang et al. 2022):

$$RP = Dk_t/(2t_t k_e) \times \ln[2(L_c + h_w - t_1 - t_2)/D] \tag{5}$$

3.3 Hydraulic status for Dublin Port Tunnel (Wang et al. 2022)

As mentioned in Wang et al. (2022), based on the derivation of the relative ground-lining permeability *RP* noted in section 3.2, the current deteriorated lining permeability for DPT, after more than a decade's operation, can be calculated using the monitored water flow data. Following the determination of lining permeability, the hydraulic deterioration status can then be assessed. To generalise the hydraulic status assessment, Figure 8 demonstrates the steps and procedures that need to be followed.

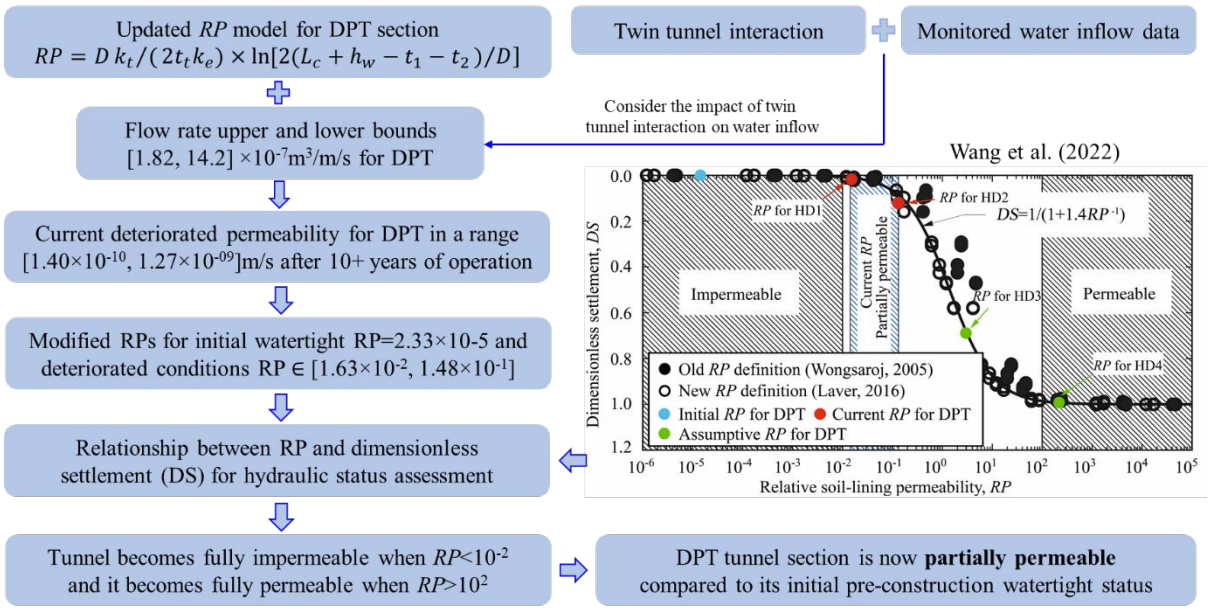

Figure 8. Generalised steps for DPT hydraulic status assessment

Considering the twin-tunnel interaction effect, the observed water flow rate for a single tunnel falls within a range of [1.82, 14.2] $\times 10^{-7}$m^3/m/s. Using this flow rate range, together with the modified relative permeability model, the current deteriorated tunnel lining permeability for the bored section of DPT is obtained as in a range within [1.40×10^{-10}, 1.27×10^{-09}]m/s after more than a decade's operation, up from the initial watertight lining permeability of 2.0×10^{-13}m/s, showing tunnel is deteriorating hydraulically with time, in agreement with previous findings by Shin et al. (2012), Bagnoli et al. (2015), Li et al. (2020), etc. Once the deteriorated tunnel lining permeability has been established, the adjusted relative ground-lining permeability *RP* for DPT can be calculated by inserting the initial permeability and deteriorated permeability of the lining into equation (5). The modified *RPs* for DPT are determined ass $RP=2.33\times10^{-5}$ and $RP \in [1.63\times10^{-2}, 1.48\times10^{-1}]$ for the initial watertight and current deteriorated conditions, respectively. Based on Laver et al. (2017)'s proposed correlation between ground-lining relative permeability *RP* and dimensionless settlement (*DS*), as demonstrated in Figure 8, initially, the *RP* value for DPT was 2.33×10^{-5} , significantly below 10^{-2}, suggesting a fully impermeable DPT lining before opening, in agreement with the design requirement being a watertight tunnel. After more than a decade of operation, the relative permeability progressively rose to a range $RP \in [1.63\times10^{-2}, 1.48\times10^{-1}]$, indicating the tunnel has begun to experience hydraulic deterioration, surpassing the threshold for

impermeable lining definition (RP<10^{-2}), and the tunnel lining is now partially permeable in comparison to its initial pre-construction condition (Wang et al. 2022). However, when compared to the surrounding ground layer's permeability of 6.10×10^{-08} m/s, the tunnel section remains relatively impermeable, with values ranging within [1.40×10^{-10}, 1.27×10^{-09}] m/s (Wang et al. 2022).

4. FINITE ELEMENT MODELLING

4.1 Three-dimensional finite element model

4.1.1 Numerical model introduction

In accordance with emergency evacuation requirements, four vehicle cross passages were constructed in Dublin Port Tunnel, with two located in the bored tunnel section. Of particular interest in this study is the VCP 16 section buried around 19.5m underneath the ground surface where the greatest mechanical and hydraulic deteriorations were observed, as shown in Figure 1(*b*) and Figure 3, compared with the other three VCP sections. Unlike underground metro twin tunnels, the twin bored urban road tunnel section features a twin layby tunnel in an irregular oval shape, spaced around 40 meters apart. These tunnels are transversely connected by a horseshoe-shaped VCP 16 for emergency evacuation and longitudinally linked by a headwall structure to the circular bored tunnel with an outer diameter of 11.22 meters, as illustrated in Figure 5 and Figure 9.

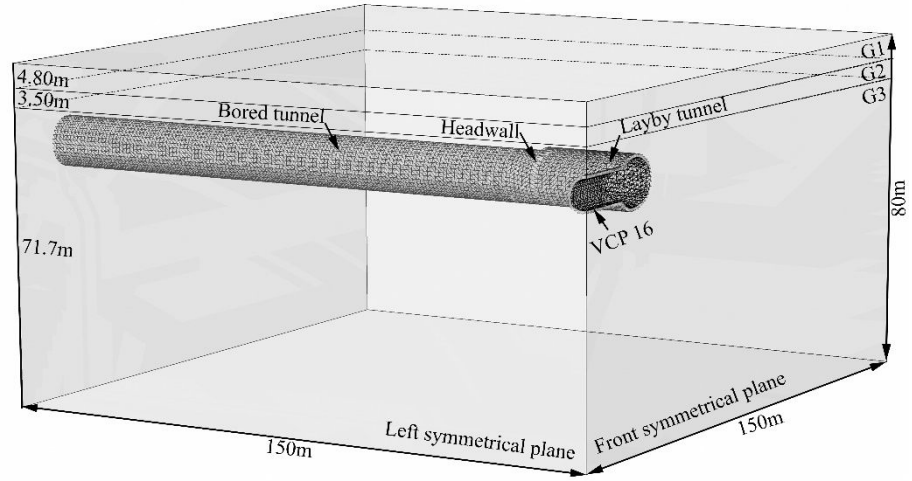

Figure 9. Finite element geotechnical model

Considering symmetrical tunnel configuration in both transverse and longitudinal directions, a quarter finite element model of the twin-tunnel cross passage section was developed. To minimise

boundary effects, the dimension of the quarter model is 150m (length) × 150m (width) × 80m (depth), which is as much as twelve times greater than the tunnel diameter. Vertical displacement at bottom of the model was fixed while the top was free. The back and right boundaries were allowed to move vertically but not perpendicularly to boundary faces, whereas the front and left surfaces were assumed as symmetrical planes (Gong et al. 2020). The vertical ground profile around the target tunnel section was shown in Figure 1(*b*) and the related physical and mechanical material properties for both ground and lining concrete were listed in Table 1. The initial pore water pressure was assumed to be hydrostatic, with the groundwater table positioned 2.0m below the ground surface.

The model was discretized using finite element analysis software ABAQUS (ABAQUS Inc. 2019) with 4-node linear coupled displacement-pore pressure tetrahedron elements (C3D4P). A finer mesh was applied at and around the tunnel structures, while a coarser mesh was used at the outer boundaries to minimise computational cost without compromising accuracy (Li et al. 2015). The layered tunnel linings were considered as one continuous layer and were all modelled using 3D continuous solid elements, which are the same element type as ground units. In addition, the concrete lining elements were connected to the adjacent ground elements at the tunnel's outer boundary using shared nodes. No specific interface was modelled, as the probability of slippage between lining and surrounding ground during tunnel operation is minimal (Wongsaroj et al. 2007). The 3D model comprised of 490,100 elements and 78,720 nodes. Considering the strength of the ground, the stress state of all ground layers should fall within the elastic range. Thus, a Mohr-Coulomb constitutive model was applied to all ground layers, while a linear elastic model was attributed to the lining concrete, so that a good balance between simplicity, computational efficiency, and adequacy for capturing the long-term structural behaviour of DPT under the influence of tunnel deteriorations can be achieved.

4.1.2 Numerical modelling sequence

On the basis of construction history, the excavation of VCP followed shortly after the construction of main tunnels (MT, i.e., bored tunnel, headwall and layby tunnel). For brevity, there are four main stages considered in numerical modelling: initial geostatic equilibrium state, MT excavation, VCP excavation and long-term operation (LTO), as detailed in Table 2.

Table 2. Modelling sequence considered in FE analyses

Stages	Stage description
1	1. Initial geostatic equilibrium state
2	2.1. Excavation of MT and MT nodal force reduction to 50% 2.2. Activation of MT linings and further MT nodal force reduction to 0%
3	3.1. Excavation of VCP and VCP nodal force reduction to 50% 3.2. Activation of VCP linings and further VCP nodal force reduction to 0%
4	4. Long-term tunnel operation for14 years from opening to 2021
5	5. Long-term tunnel operation for another 20 years from 2021

After initial geostatic equilibrium state, the excavation of twin tunnels was modelled by removing the MT linings and the ground inside first, followed by the application of nodal force around MT external circumference. To simulate the stress redistribution after MT excavation and the time lag before the installation of tunnel linings, the equivalent nodal forces were relaxed to 50% of its original magnitude, with subsequent placement of linings and another nodal force reduction of 50% thereafter (Li et al. 2015). The same process was also adopted for VCP excavation before long-term operation begins. As this study focuses on the long-term performance of DPT under the influence of deteriorations, the modelling of tunnel excavation process and the immediate subsequent support installation was assumed to be short-term (occur rapidly), minimising drainage during this period. Therefore, it was assumed that all construction stages were simplified to took place under undrained conditions to save computational cost. In the long-term post-construction stage, tunnel drainage was allowed. Water flow into the tunnel is only enabled in ABAQUS when a drainage-only boundary is specified. When the pore water pressure becomes negative, the inflow ceases because no water is supplied from the tunnel to the surrounding ground, enhancing the practicality and realism of numerical simulations regarding ground-tunnel drainage conditions (Li et al. 2015).

4.2 Modelling the impact of deteriorations

4.2.1 Modelling tunnel hydraulic deterioration

After tunnel construction, the presence of lining structures may create different types of new drainage boundaries within the ground depending on the permeability difference between adjacent ground and tunnel lining. As mentioned in section 1, two hydraulic scenarios may occur during post-construction tunnel operation: (1) the blockage of water drainage system around tunnel lining (Di Murro 2019); (2) the cracking/construction joint expansion-induced water seepage or infiltration into tunnels (Shin et al. 2012). To model how such two hydraulic deteriorations affect tunnel performance, clogged drainage system is simulated by decreasing the coefficient of tunnel lining permeability whilst cracking-induced water leakage is modelled by the increase of lining permeability (Shin et al. 2012). However, no sign of groundwater drainage system blockage has been reported since DPT operation. Only water infiltration caused by crack/joint initiation and propagation is therefore considered in this study by increasing lining permeability. Using the deteriorated lining permeability obtained in section 3, a series of hydro-mechanical coupled numerical simulations is carried out to assess the ageing responses of DPT under the influence of time-dependent hydraulic deteriorations during the first 14 years of operation. With time, it is projected tunnel hydraulic deteriorations will continue and therefore it is assumed that the tunnel section will become increasingly permeable in the next two decades. The scenarios considered in this simulation are listed in Table 3. HD1 represents the scenario where lining permeability remains almost unchanged since 2021 (the lower bound) whilst HD4 represents the worst case of hydraulic deterioration after the 14-year operation (the upper bound: the tunnel section becomes fully permeable in the next decades (e.g., 20 years of operation)).

The *RP*s for these assumptive scenarios for DPT are included in Figure 8 to illustrate the tunnel lining hydraulic status for these cases (becoming increasingly permeable). The tunnel lining is designed to be watertight throughout its service lifetime of 120 years. To save computational resources, to capture the overall impact of hydraulic deterioration on the general trends of tunnel long-term performance, and to bypass the challenges associated with measuring and incorporating detailed crack/joint distribution and characteristics, a uniform liner permeability is applied to tunnel lining before and after deterioration.

An initial value of 2.0×10^{-13}m/s is allocated to all sections of the tunnel lining. With time, the cracking-induced tunnel lining permeability increases. Many previous studies proposed some representative analytical models to model the increase of lining permeability, with most models established based on the evolution of crack interconnection and propagation and concrete corrosion (Li et al. 2020). However, in reality, the evolution of lining permeability can be attributed to various factors which can be physical, chemical or biological. It is unlikely to single out the exact cause of cracking-induced liner hydraulic deterioration and difficult to characterise the evolution law of lining concrete permeability under the influence of a particular factor, without comprehensive tests or monitoring. Therefore, on account of the absence of field data and by referencing the observed trends in concrete deterioration reported in some previous studies (Han and Jeong 2014; Sandrone and Labiouse 2010), the lining permeability of the tunnel section in question is presumed to rise linearly over the 14-year operational period from the initial watertight value to the current deteriorated value by the end of this period, to simplify the modelling process and provide a practical way to simulate progressive lining hydraulic deterioration (Li et al. 2020). The same law is also assumed to be applicable to the increase of lining permeability from the deteriorated value to a more permeable status during the next 20 years.

Table 3. Tunnel lining hydraulic deterioration scenarios

Scenarios		k_t before long-term operation	k_t after first 14 years of operation	k_t after another 20 years of operation
Hydraulic Deteriorations (HD group)	HD1	2.00×10^{-13}m/s	1.40×10^{-10}m/s	1.40×10^{-10}m/s
	HD2	2.00×10^{-13}m/s	1.40×10^{-10}m/s	1.27×10^{-09}m/s
	HD3	2.00×10^{-13}m/s	1.40×10^{-10}m/s	1.27×10^{-08}m/s
	HD4	2.00×10^{-13}m/s	1.40×10^{-10}m/s	1.27×10^{-07}m/s

4.2.2 Modelling tunnel mechanical deterioration

As mentioned, in addition to hydraulic deteriorations, Dublin Port Tunnel has also been observed with some mechanical deterioration, exemplified by concrete lining cracking and spalling. The time-dependent mechanical deterioration contributes to the reduction of lining mechanical properties. For

DPT, the middle section of the tunnel was excavated using a Tunnel Boring Machine where the segmental lining was constructed as the primary liner. To consider the presence of tunnel joints, the equivalent stiffness of the tunnel lining ring can be obtained through applying a stiffness reduction factor to segment stiffness, as demonstrated in many previous studies (Li et al. 2015; Lu et al. 2020; Ye and Liu 2021; Zhang et al. 2015). Muir Wood's formula, $I_e=I_j+I\times(4/n)^2$, is commonly adopted to calculate the factor but is only applicable to segmental lining with identical segments.

For other non-identical segmental tunnels, similar values of reduction factors were also assumed previously. Li et al. (2015) assumed a reduction factor of 0.44 for old segmental cast-iron linings, Zhang et al. (2015) chose a 0.6 for a Shanghai segmental tunnel, Lu et al. (2020) and Ye and Liu (2021) gave a value of 0.7 for their respective segmental tunnels. Similarly, for DPT, an assumed reduction factor of 0.5 for the original segment stiffness of 30GPa is adopted to calculate the equivalent stiffness of the tunnel lining ring.

Typically, tunnel mechanical deterioration is simulated by reducing the stiffness of the concrete lining. However, due to the uncertainty in singling out the exact cause of the mechanical deterioration, it is not likely to quantitatively determine the degree of lining stiffness reduction, but previous work has offered some insights into the evolution of Young's modulus of concrete lining (Nguyễn 2005; Sandrone and Labiouse 2010):

$$\delta E / E_0 = (E_0 - E) / E_0 = k_m \times \delta d \tag{6}$$

where E_0 represents the original Young's modulus of tunnel lining ring, while k_m is 0.66 for a medium-quality concrete; δd represents the ratio of deteriorated depth to the initial thickness, i.e., $\delta d = X_d/ds$. Usually, the deteriorated thickness, X_d, is considered proportional to the square root of time t:

$$X_d = a \times \sqrt{t} \tag{7}$$

The deterioration rate, a, is a material constant which depends on the external environment and concrete quality. The deterioration of the thickness of tunnel lining due to Calcium leaching, for example, in an underground environment, can reach a maximum value of 100 to 120 mm in 100 years (Showkati et al. 2021; Yokozeki et al. 2004), which gives the estimated deterioration rate a range of $[5.0 \sim 6.0] \times 10^{-4}$ (m/√days). In the case of DPT, the reduction of tunnel lining stiffness is believed to be caused by the

coupling of lining cracking & spalling and water ingress, which presumably could lead to a higher rate of deterioration. Therefore, a higher rate of 1.0×10^{-03}m/√days is assumed as the upper bound for the modelling of DPT mechanical deterioration during both the first 14 years and the second 20 years, and a smaller rate of 5.0×10^{-04} m/√day is assumed as the lower bound for the two durations. In this study, to simplify the numerical simulation process and due to the difficulty in characterising the evolution law of lining Young's modulus under the influence of a particular influencing factor without comprehensive tests or monitoring data, the mechanical deterioration of the lining is simulated by a linear reduction of lining stiffness with time during the modelling period, based on similar trends of concrete deterioration reported in previous studies (Liu et al. 2023; Zhang et al. 2024).

4.3 Field and numerical results comparison

4.3.1 Effect of lining deteriorations

Influence of lining hydraulic deterioration

Figure 10 illustrates the time-dependent progression of convergence for a complete lining ring located on the layby, positioned 7 meters from the front symmetrical plane as depicted in Figure 5. The analysis covers hydraulic deterioration scenarios outlined in Table 3, commencing from the year 2021. As the tunnel lining becomes increasingly permeable, the layby tunnel section experiences greater deformation in both vertical and horizontal directions, with vertical deformation exceeding horizontal deformation. The maximum horizontal convergence (~1.1mm) accounts for approximately 30% of the maximum vertical diameter change (~3.8mm) on average. When the tunnel section remains in an undeteriorated state starting from 2021, it can be seen its deformation was observed with fast shrinkage in the first few months and then stabilised thereafter, as shown in Figure 10(a), which could be attributed to the fast arrival of a new steady hydraulic state. In comparison, when the tunnel becomes more and more permeable, the tunnel deformation develops with time, as shown in Figure 10(b-d), rendering a sharp contrast with what was observed in Figure 10(a). The difference suggests that assuming a constant hydraulic permeability throughout tunnel operation may not accurately portray the time-dependent tunnel deformation process in a realistic manner.

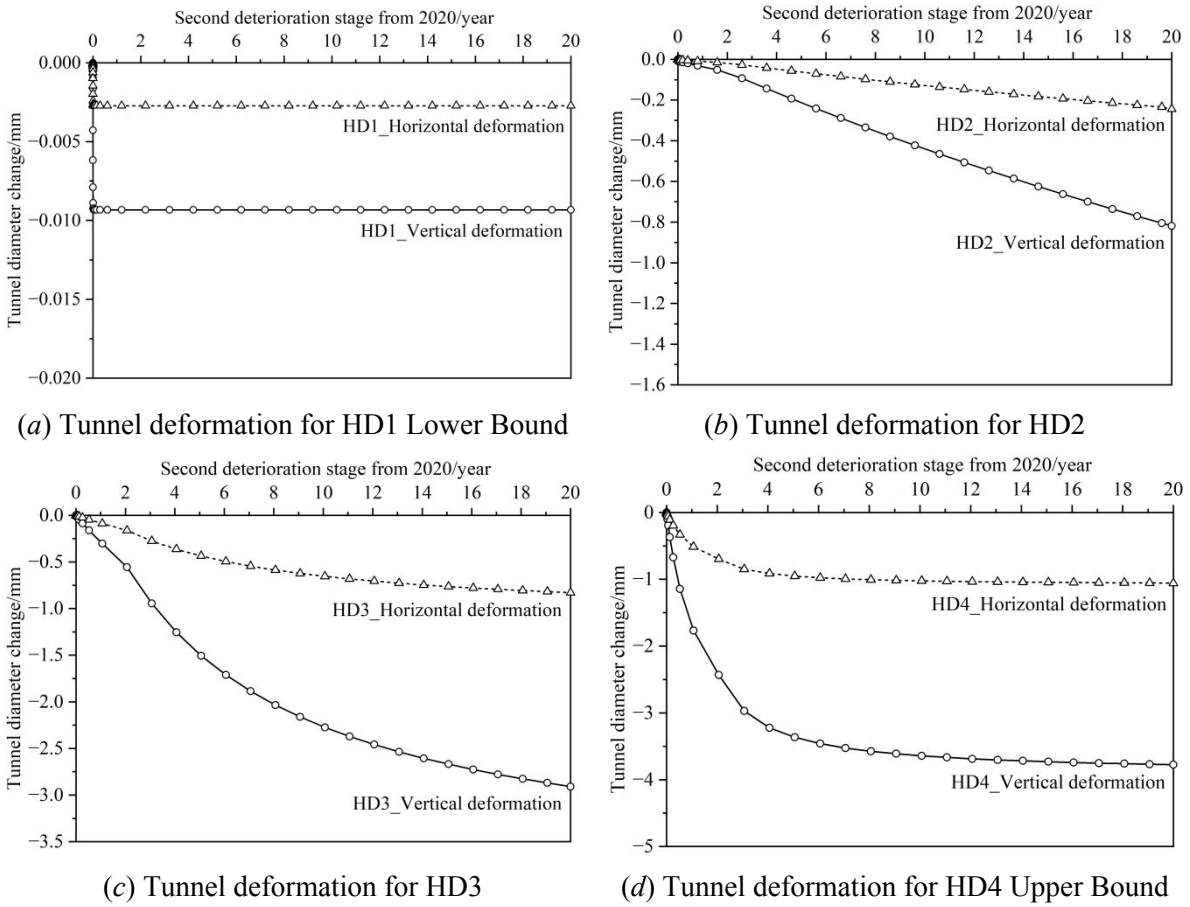

(*a*) Tunnel deformation for HD1 Lower Bound (*b*) Tunnel deformation for HD2

(*c*) Tunnel deformation for HD3 (*d*) Tunnel deformation for HD4 Upper Bound

Figure 10. Tunnel deformation development induced by lining hydraulic deterioration (HD)

Taking the deterioration/ageing process into consideration brings more insights into how tunnel structure behaves with time during its lifetime in greater depth for tunnel maintenance. To understand how hydraulic deterioration influences the deformation mode of the tunnel section, Figure 11(a) illustrates the deformation profiles of the liner ring shown in Figure 5 under different hydraulic deterioration scenarios listed in Table 3. As the tunnel lining becomes increasingly permeable, the twin layby tunnels move towards each other, undergoing a squatting contraction deformation mode, as shown in Figure 11(b). This deformation mode aligns with the mode from field measurements reported by Wang et al. (2023). This observation can be attributed to twin tunnel interaction effect where the ground in between the twin tunnels has shorter drainage paths than the ground at the sides of the twin tunnels and this causes retraction of horizontal support for tunnel sections close to the middle ground, leading to an increasing horizontal movement of tunnel linings towards the middle ground while undergoing squatting deformation Wang et al. (2023).

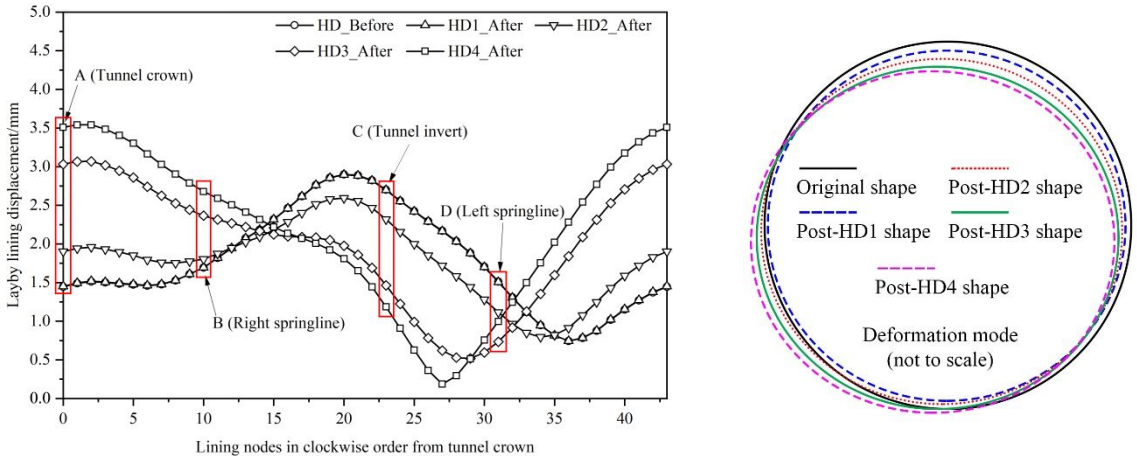

(*a*) Tunnel deformation profiles (*b*) Tunnel deformation modes

Figure 11. Hydraulic deterioration induced tunnel deformation profiles and modes

Influence of lining mechanical deterioration

Figure 12 shows the development of deformation induced by lining mechanical deterioration with time. The deformation of the tunnel increases over time, with the vertical diameter change (maximum of 0.17mm) exceeding the horizontal convergence change (maximum of 0.11mm). This indicates a contraction with a squatting deformation mode. With the continuous deterioration of concrete lining, both diameters decrease approximately linearly with time. Figure 13 illustrates the deformation profiles and modes of the lining ring of interest under the influence of mechanical deteriorations. It can be seen that the mechanical deterioration of concrete lining induces an inward convergence of the lining in an almost isotropic way (Xiao et al. 2023) but with the most deformation occurring in the upper part of the lining. The mechanical deterioration-induced tunnel deformation could be associated with reduced ability to support ground pressure and external loads, which hinders effective load transfer from lining to the surrounding ground, contributing to increasing lining internal forces and deformation.

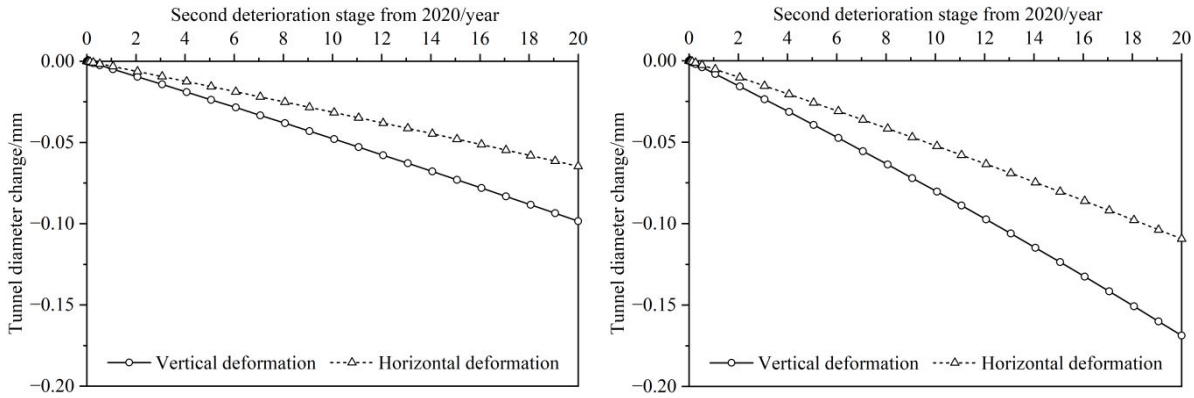

(*a*) MD-induced deformation-Lower Bound (*b*) MD-induced deformation-Upper Bound

Figure 12. Tunnel deformation development induced by lining mechanical deterioration (MD)

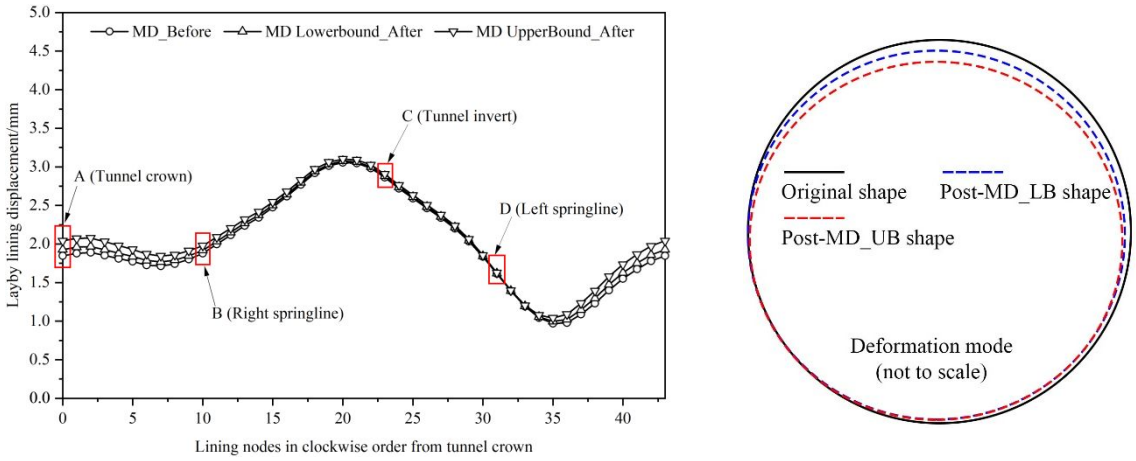

(*a*) Tunnel deformation profiles (*b*) Tunnel deformation modes

Figure 13. Mechanical deterioration induced tunnel deformation profiles and modes

Influence of coupled lining deterioration

As mentioned earlier, the selected tunnel section has been observed with both mechanical and hydraulic deteriorations exemplified by lining cracking and water leakage. The influence of the two deteriorations has been numerically investigated individually. Practically, tunnel deterioration occurs concurrently instead of individually and the two deteriorations occur in no specific order. To this end, a further series of finite element analyses is conducted to assess the influence of the coupled deterioration on the long-term performance of the tunnel. By coupling lining hydraulic deterioration and mechanical deterioration, Table 4 lists the upper bound (UB) and lower bound (LB) cases for simulation. It should be noted that tunnel mechanical deterioration starts concurrently in both hydraulic deterioration stages.

Figure 14 shows the development of layby tunnel deformation with time under the impact of coupled tunnel hydro-mechanical deteriorations. It is obvious that the deformation tendencies observed in coupled deterioration cases are similar to the ones captured in hydraulic deterioration and mechanical

Table 4. Simulation cases for coupled lining deteriorations

Scenarios	Hydraulic deterioration (k_t increase)		Mechanical deterioration (deterioration rate a)
	First 14 years	Second 20 years	

CD1_LB	2.0×10^{-13}~1.40×10^{-10}m/s	1.40×10^{-10}m/s~1.40×10^{-10}m/s	a=5.0×10^{-04}
CD2_UB		1.40×10^{-10}m/s~1.27×10^{-07}m/s	a=1.0×10^{-03}

deterioration cases. For instance, the deformation tendency in CD2 is similar to that in HD4, and another similar trend was found between CD1 and MD1. Regarding the magnitude of tunnel deformation, such coupling indeed exacerbates tunnel deformation as confirmed by the greater deformation (maximum c.a. 4.2mm vertical convergence and c.a. 1.4mm horizontal convergence for CD scenarios) than that obtained from modelling the individual impact in Figure 10 (the maximum horizontal convergence of ~1.1mm and maximum vertical diameter change of ~3.8mm for HD cases) and Figure 12 (max value of 0.17mm vertical convergence and max value of 0.11mm for horizontal one for MD cases). Figure 15 illustrates the deformation profiles and modes of the tunnel section under the influence of coupled deteriorations. It can be seen that the deformation mode under the influence of coupled deterioration is the same as that observed in hydraulic deterioration (Figure 11(b)), indicating hydraulic deterioration is the dominating factor in the coupled deterioration that contributes to the ongoing tunnel deformation and mechanical deterioration only plays a very limited role.

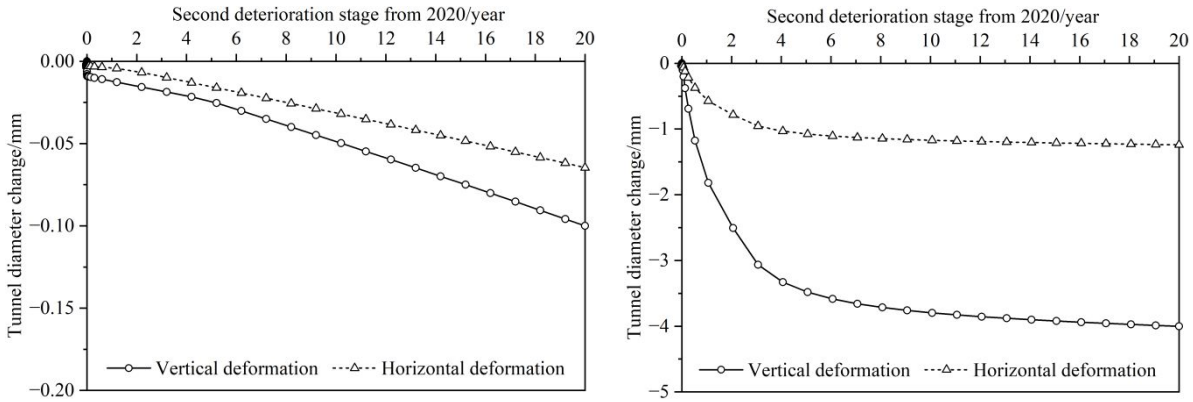

(*a*) CD-induced deformation-Lower Bound (*b*) CD-induced deformation-Upper Bound

Figure 14. Tunnel deformation development induced by coupled lining deterioration (CD)

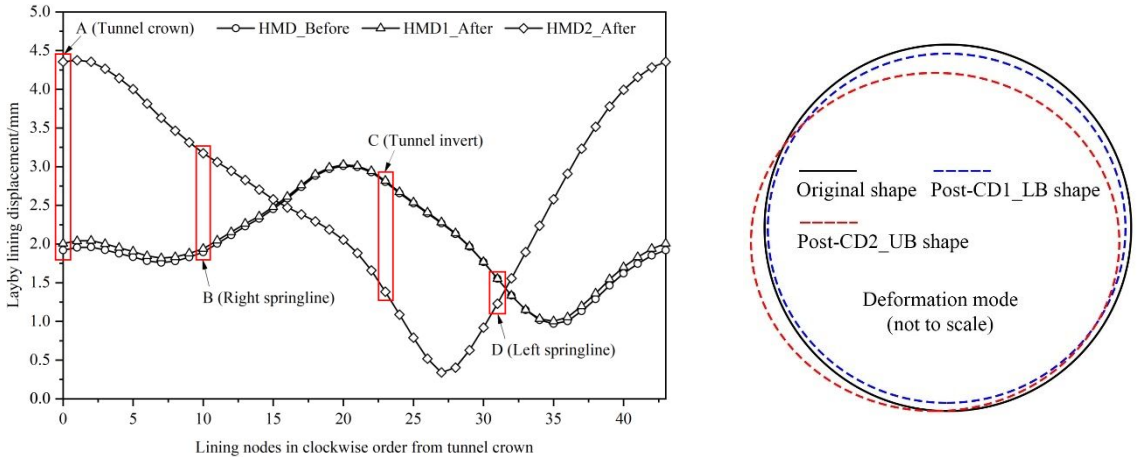

(*a*) Tunnel deformation profiles (*b*) Tunnel deformation modes

Figure 15. Coupled hydro-mechanical deterioration induced tunnel deformation profiles and modes

4.3.2 Numerical and field data comparison

To compare the numerical results and field data of DPT performance, the horizontal deformation rate is chosen as the index for the numerical model validation. Due to the fact that the selected deteriorations fall within a range, it is assumed that the numerical model is validated when the monitored rate of tunnel horizontal deformation falls within the range of deformation rate obtained from numerical studies with the worst and best scenarios, and when the deformation mode obtained from numerical studies remains consistent with that from field measurement. The numerical results from the first two years of the second deterioration stage (20 years) starting from 2021 are compared against the field measurements collected during the first two years of monitoring from summer 2021 that are available in Wang et al. (2023), in order to eliminate the impact of season difference on calculating tunnel deformation rate.

According to Wang et al. (2023), a system of wireless sensor network (WSN) inclinometers was deployed at the VCP 16 cross-passage twin tunnel section, as illustrated in Figure 16. Two central rings of the layby tunnel were mounted with three inclinometers on each as they are anticipated to develop the maximum deformation due to VCP 16 opening. Another two rings of inclinometers were deployed at tunnel sections with the most deteriorations. The monitoring started in summer 2021 with a sampling frequency of every 60mins. All monitoring data were transmitted wirelessly to the cloud before being downloaded for post processing. The monitored tilt data were converted to cross-sectional deformation based on derivation proposed in Wang et al. (2023) for comparison against numerical results. Figure 17

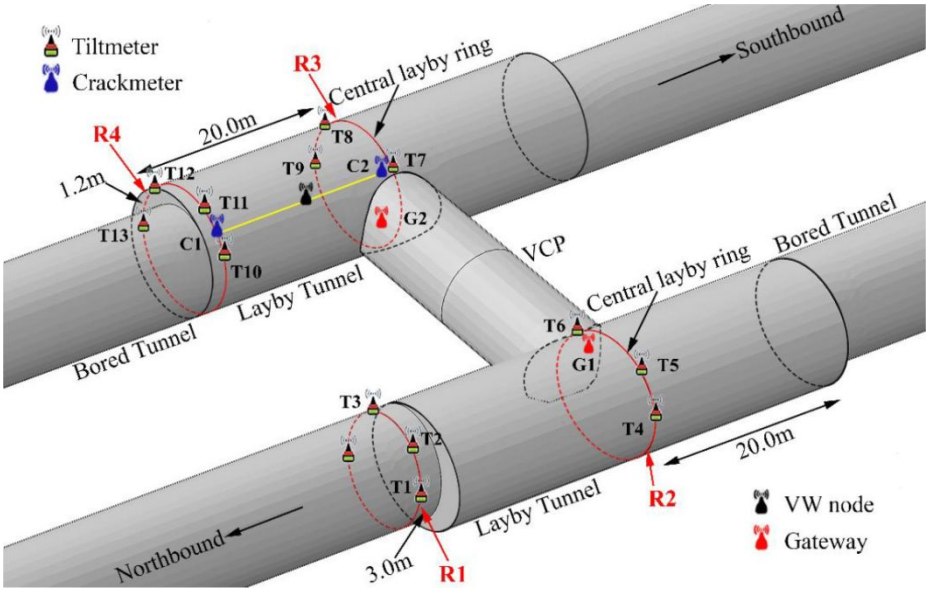

Figure 16. WSN sensor deployment at VCP 16 section (Wang et al. 2023)

compares the rate of horizontal deformation obtained from both numerical results under the influence of different lining deterioration and field monitoring data. It can be seen from Figure 17(*a*) that the field rate of tunnel horizontal deformation captured in Wang et al. (2023) generally falls within the range of deformation rate obtained from simulating the influence of tunnel hydraulic deterioration, except for a few monitoring locations (e.g., T4 and T9), indicating that lining hydraulic deterioration may be a dominant factor leading to the ongoing and increasing tunnel deformation. Upon comparison, Figure 17(*b*) shows that the maximum rate of tunnel deformation under the influence of liner mechanical deterioration is still smaller than the rate obtained from field monitoring. The difference between the numerical and field rate of deformation suggests tunnel mechanical deterioration only plays a limited role in causing the long-term deformation of the tunnel. However, as shown in Figure 17(*c*), it is obvious that the field rate of tunnel deformation falls within the range of the rate of tunnel deformation derived from simulating the coupled hydraulic-mechanical deterioration of tunnel lining, indicating the ongoing and increasing tunnel deformation observed from field data can be attributed to the coupled influence of tunnel hydraulic and mechanical deteriorations, instead of the influence of individual deterioration, and lining hydraulic deterioration induces a majority of observed lining deformation.

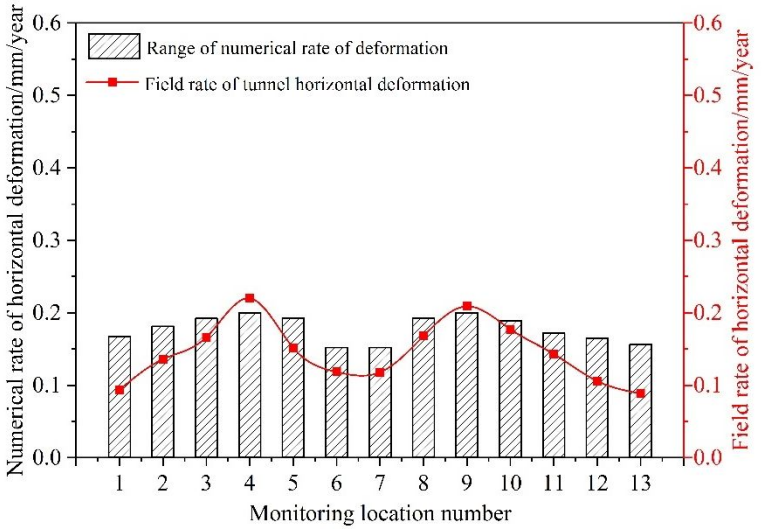

(*a*) Influence of lining hydraulic deterioration

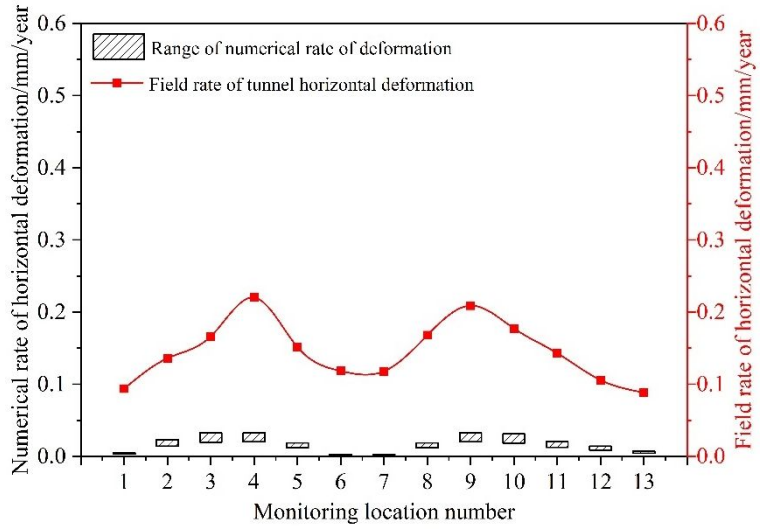

(*b*) Influence of lining mechanical deterioration

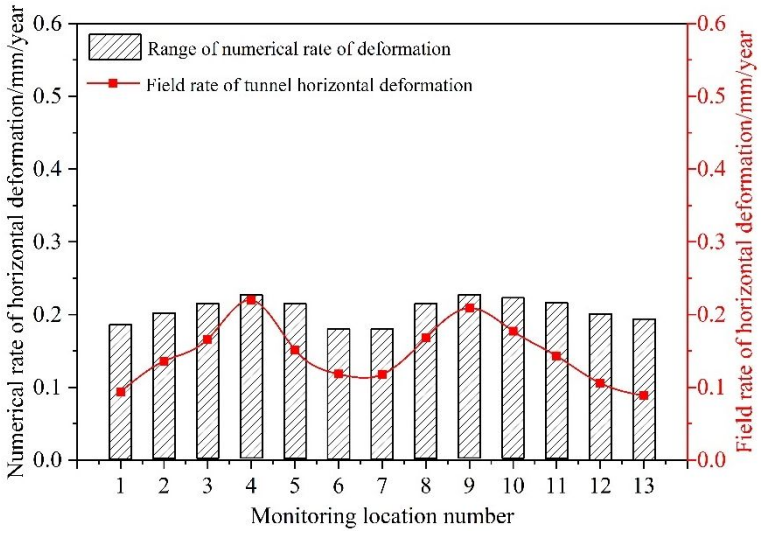

(*c*) Influence of coupled lining deterioration

Figure 17. Comparison of numerical and field deformation rates under various deteriorations

Figure 18 shows the rate, direction and tendency of tunnel deformation from both field monitoring and coupled deterioration modelling (blue arrow represents the direction of horizontal movement; red arrow shows the tilting direction of the monitored location). It is clear the direction of horizontal movement observed in numerical simulation is in agreement with the direction observed in WSN field monitoring presented in Wang et al. (2023). In addition, both field data and numerical results demonstrate that (1) generally, the rate of deformation for monitoring locations on the two central rings R2 and R3 is comparatively higher than the rate for the corresponding locations on the other two rings R1 and R4, except for the locations within the interaction zone (T6 and T7) due to the horizontal pushback by soil loading at the VCP-layby connection junction; (2) the rate of deformation at locations T3 on lining ring R1 and T10, T11 on lining ring R4 is greater than the rate at other locations on the same ring (T1 & T2 on ring R1, T12 & T13 on ring R4), due to the influence of twin tunnel interaction on liner section close to the ground in-between the two tunnels. It is also noticeable that the difference in the magnitude of deformation rate on R1 and R4 obtained from numerical studies is small, which could be attributed to the assumption of uniformly distributed deteriorations of the tunnel liner along both circumferential and longitudinal directions. Based on the agreement between the field measurements and numerical results obtained above, it is therefore reasonable to conclude that the numerical model is validated.

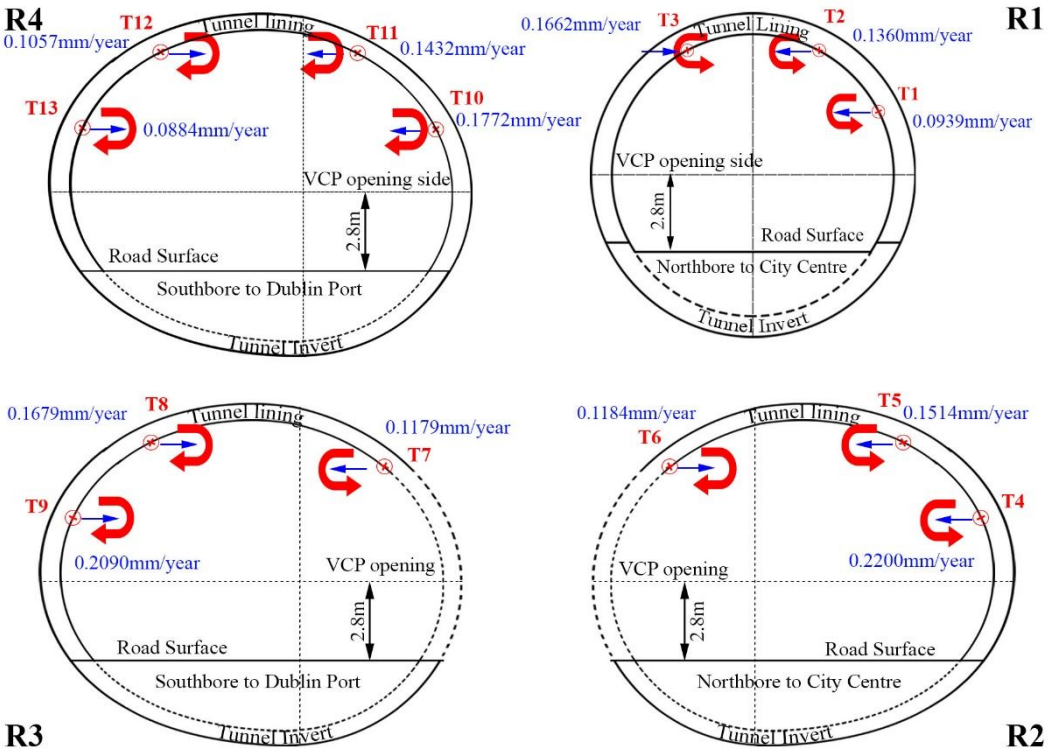

(*a*) Field results Wang et al. (2023)

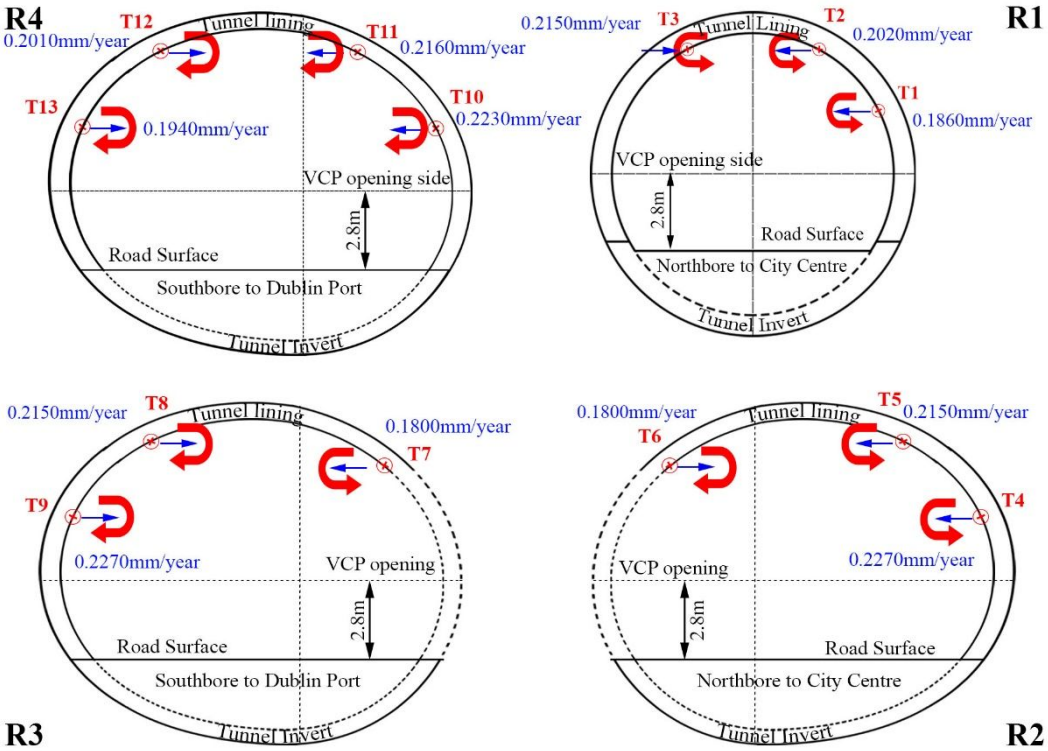

(*b*) Numerical results (worst CD case)

Figure 18. Rate, direction and tendency of tunnel deformation

5. DISCUSSIONS AND CONCLUSIONS

5.1 Discussions

This study underscores the critical importance of modelling the effect of time-dependent hydraulic and mechanical deterioration processes on DPT's long-term performance. By addressing the gaps and limitations in previous models, this study provided a validated and integrative approach to tunnel deterioration. Through integrating deteriorated lining permeability into hydraulic deterioration model, together with mechanical deterioration, a more accurate prediction of tunnel long-term performance is obtained, and a comprehensive framework that integrates various deterioration mechanisms is presented. The validation of the model with field measurements enhances the credibility of the model and findings, making it a valuable tool for practitioners. The findings are of reference for ensuring structural integrity, safety, and serviceability, thereby improving DPT's risk management and maintenance planning.

While Dublin Port Tunnel served as a specific case study, our methodology can be generalised and broadly applied to various tunnel scenarios. Practitioners can adapt the model by calibrating parameters to local geotechnical conditions, construction techniques, and observed deterioration patterns. This adaptability ensures that the model serves as a versatile tool for different tunnel types, enhancing its utility in diverse engineering contexts. In addition, our findings also offer some practical insights for asset management. The modelling and monitoring results of the cross-passage twin tunnel section of DPT both showed the critical deformation at the VCP opening junction, which can be of reference to future tunnels with similar configurations. These results suggest optimising the design and construction at such critical locations of new tunnels can help prevent the occurrence of significant deformation, and for operating tunnels, these results can be insightful for practitioners to predict potential problem areas such as areas with cross passages and thus prioritise inspections and implement targeted maintenance and repair strategies.

In this study, both hydraulic and mechanical deteriorations were assumed to continue developing during the specific timeframes under simplifying conditions. Realistically, their developments, either during the investigated timeframes or beyond, are subject to the influence of various factors like groundwater conditions, external disturbances, and maintenance intervention. Understanding their

developments based on field measurements is critical to accurately predict tunnel long-term behaviour. The field monitoring mentioned is expected to continue into the future. Thus, long-term monitoring and adaptive modelling are recommended to adjust predictions as new data becomes available.

Apart from the significance and implications, it is worthy of noting that there are a few limitations in this study, including simplified assumptions in the derivation of deteriorated lining permeability like isotropic ground and lining permeability and constant groundwater table, simplified assumptions in modelling lining deterioration such as uniform permeability and linear deterioration which may not capture all localised effects of deteriorations, and the lack of comprehensive (e.g., spatially continuous data) and even longer-term field data for more precise model validation. Future studies should consider the impact of more localised deteriorations and test data-based deterioration development and/or aim to incorporate additional deterioration processes like sulphate attack and carbonation of concrete, physical deterioration featured by freeze-thaw cycles, groundwater erosion, and chloride-induced reinforcement corrosion. Addressing these areas can further advance our understanding of the long-term performance of tunnels in a more realistic and comprehensive manner.

5.2 Conclusions

Understanding how tunnel deteriorations affect the long-term performance of tunnel structures remains imperative, with many previous studies overlooking the time-dependent nature of these deteriorations. Using Dublin Port Tunnel as a case study, this paper firstly presents the general steps and processes for deriving a modified relative permeability model and calculating the deteriorated hydraulic permeability of DPT, followed by assessing its hydraulic deterioration status. More importantly, by incorporating time-dependent hydraulic and mechanical deteriorations, the 3D finite element geotechnical model was validated through comparing numerical results against field measurements. The main conclusions and key contributions are summarised as follows:

(1) The modified analytical relative ground-lining permeability model for DPT proposed before has now been extensively validated against field measurements from Dublin Port Tunnel. The calculated deteriorated hydraulic permeability of DPT was incorporated into the hydraulic deterioration model, together with mechanical deterioration, providing a more holistic and realistic prediction of the

long-term performance of DPT than previously available. The new model provides a new tool for accurate assessment of the hydraulic deterioration condition of ageing tunnels.

(2) Assuming constant hydraulic permeability throughout tunnel operation fails to realistically portray time-dependent tunnel deformation. By considering the ageing process, this study brings deeper insights into tunnel long-term performance. The study identifies hydraulic deterioration as inducing an approaching squatting deformation mode with slight settlement, consistent with field measurements. This observation can be attributed to twin tunnel interaction effect where the shorter drainage path of the ground in between the twin tunnels causes retraction of horizontal support for tunnel sections close to the middle ground, leading to an increasing horizontal movement of tunnel linings towards the middle ground while undergoing squatting deformation.

(3) Continuous tunnel mechanical deterioration leads to an increase in tunnel deformation in both directions, with vertical convergence being greater than the horizontal one. This results in a contraction but squatting deformation mode, with inward convergence of the lining being almost isotropic but more pronounced in lining's upper part. Such deformation observations could be associated with reduced ability to support ground pressure and external loads, which hinders effective load transfer from lining to the surrounding ground, contributing to increasing lining deformation.

(4) The comparison between the numerical results obtained from the individual deterioration effect and field data shows the effect of lining hydraulic deterioration plays a dominant role in leading to the observed ongoing tunnel deformation but the effect of lining mechanical deterioration only plays a very limited role. Instead, the coupled hydraulic-mechanical deterioration of the tunnel liner leads to greater tunnel deformation than individual deterioration does. Both field measurements and numerical results demonstrated: generally, the rate of deformation on the two central rings R2 and R3 is comparatively higher than the rate on the other two rings R1 and R4, except for locations within the interaction zone (T6 and T7) due to the horizontal pushback by soil loading at the VCP-layby connection junction; the rate of deformation at locations T3 on lining ring R1 and T10, T11 on lining ring R4 is greater than the rate at other locations on the same ring (T1 & T2 on ring R1, T12 & T13 on ring R4), due to the influence of twin tunnel interaction on liner section close to the ground in-between the two tunnels. The

agreement between the field data and numerical results confirms that coupled lining deterioration is the root cause behind the monitored lining deformation.

STATEMENTS AND DECLARATIONS

DATA AVAILABILITY

Some or all data, models, or code that support the findings of this study are available from the corresponding author upon reasonable request.

DECLARATION OF COMPETING INTEREST

The authors declare that they have no known competing financial interests or personal relationships that could have appeared to influence the work reported in this paper.

ACKNOWLEDGEMENT

We appreciate the joint funding by iCRAG (Irish Centre for Research in Applied Geosciences) of Science Foundation Ireland and Transport Infrastructure Ireland. It is greatly appreciated Geological Survey Ireland and Egis Road and Tunnel Operation contributed the geotechnical and mechanical data that are necessary for numerical modelling. We also thank Professor Mike Long from University College Dublin for facilitating the project and the sponsorship from National Natural Science Foundation of China (No. 51978530).

AUTHOR CONTRIBUTIONS

Chao Wang: Conceptualisation, Methodology, Formal analysis, Investigation, Writing - Original Draft.

Zhipeng Xiao: Methodology, Formal analysis, Writing - Review & Editing

Miles Friedman: Writing - Review & Editing, Supervision, Project administration, Funding acquisition.

Zili Li: Conceptualisation, Writing - Review & Editing, Supervision, Funding acquisition.

REFERENCE

Bagnoli, P., Bonfanti, M., Della Vecchia, G., Lualdi, M., Sgambi, L. 2015. A method to estimate concrete hydraulic conductivity of underground tunnel to assess lining degradation. Tunnelling and Underground Space Technology 50, 415-423.

Cabarkapa, Z., Milligan, G.W.E., Menkiti, C.O., Murphy, J., Potts, D.M. 2003. Design and performance of a large diameter shaft in Dublin Boulder Clay, BGA International Conference on Foundations: Innovations, observations, design and practice, pp. 175-185.

Di Murro, V. 2019. Long-term performance of a concrete-lined tunnel at CERN, Department of Engineering. University of Cambridge, Cambridge, UK.

Gong, C., Ding, W., Xie, D. 2020. Twin EPB tunneling-induced deformation and assessment of a historical masonry building on Shanghai soft clay. Tunnelling and Underground Space Technology 98, 103300.

Han, Y.-C., Jeong, S. 2014. A Study on the Concrete Lining Behavior due to Tunnel Deterioration. Journal of the Korean Geotechnical Society 30.

Idris, J., Al-Heib, M., Verdel, T. 2009. Numerical modelling of masonry joints degradation in built tunnels. Tunnelling and Underground Space Technology 24, 617-626.

Kim, K.-H., Park, N.-H., Kim, H.-J., Shin, J.-H. 2020. Modelling of hydraulic deterioration of geotextile filter in tunnel drainage system. Geotextiles and Geomembranes 48, 210-219.

Kovacevic, N., Miligan, G.W.E., Menkiti, C.O., Long, M., Potts, D.M. 2008. Finite element analyses of steep man-made cuts in Dublin boulder clay. Canadian Geotechnical Journal 45, 549-559.

Laver, R.G., Li, Z., Soga, K. 2017. Method to Evaluate the Long-Term Surface Movements by Tunneling in London Clay. Journal of Geotechnical and Geoenvironmental Engineering 143, 06016023.

Laver, R.G., Soga, K., Wright, P., Jefferis, S. 2013. Permeability of aged grout around tunnels in London. Géotechnique 63, 651-660.

Lawler, M.L., Farrell, E.R., Lochaden, A.L.E. 2010. Comparison of the measured and finite element–predicted ground deformations of a stiff lodgement till. Canadian Geotechnical Journal 48, 98-116.

Lehane, B.M., Simpson, B. 2000. Modelling glacial till under triaxial conditions using a BRICK soil model. Canadian Geotechnical Journal 37, 1078-1088.

Li, W., Afshani, A., Akagi, H., Oka, S. 2020. Influence of lining permeability and temperature on long-term behavior of segmented tunnel. Soils and Foundations 60, 425-438.

Li, Z., Soga, K., Wright, P. 2015. Long-term performance of cast-iron tunnel cross passage in London clay. Tunnelling and Underground Space Technology 50, 152-170.

Liu, C., Zhang, D., Zhang, S., Fang, Q., Sun, Z. 2023. Long-term mechanical analysis of tunnel structures in rheological rock considering the degradation of primary lining. Underground Space 10, 217-232.

Long, M., Menkiti, C. 2007a. Characterisation and engineering properties of Dublin Boulder Clay. Characterisation and Engineering Properties of Natural Soils 3, 2003-2045.

Long, M., Menkiti, C.O. 2007b. Geotechnical properties of Dublin Boulder Clay. Géotechnique 57, 595-611.

Lu, D., Li, X., Du, X., Lin, Q., Gong, Q. 2020. Numerical simulation and analysis on the mechanical responses of the urban existing subway tunnel during the rising groundwater. Tunnelling and Underground Space Technology 98, 103297.

Nguyễn, V.H. 2005. Couplage dégradation chimique - comportement en compression du béton. École des Ponts ParisTech, Paris.

Picandet, V., Khelidj, A., Bellegou, H. 2009. Crack effects on gas and water permeability of concretes. Cement and Concrete Research 39, 537-547.

Sandrone, F., Labiouse, V. 2010. Analysis of the evolution of road tunnels equilibrium conditions with a convergence–confinement approach. Rock Mechanics and Rock Engineering 43, 201-218.

Shin, J.-H., Kim, S.-H., Shin, Y.-S. 2012. Long-term mechanical and hydraulic interaction and leakage evaluation of segmented tunnels. Soils and Foundations 52, 38-48.

Shin, J.H., Potts, D.M., Zdravkovic, L. 2005. The effect of pore-water pressure on NATM tunnel linings in decomposed granite soil. Canadian Geotechnical Journal 42, 1585-1599.

Showkati, A., Salari-rad, H., Hazrati Aghchai, M. 2021. Predicting long-term stability of tunnels considering rock mass weathering and deterioration of primary support. Tunnelling and Underground Space Technology 107, 103670.

Sivakugan, N., Das, B.M., Lovisa, J., Patra, C.R. 2014. Determination of c and φ of rocks from indirect tensile strength and uniaxial compression tests. International Journal of Geotechnical Engineering 8, 59-65.

Skipper, J., Follett, B., Menkiti, C.O., Long, M., Clark-Hughes, J.J.Q.J.o.E.G., Hydrogeology 2005. The engineering geology and characterization of Dublin Boulder Clay. Quarterly Journal of Engineering Geology and Hydrogeology 38, 171 - 187.

Usman, M., Galler, R. 2013. Long-term deterioration of lining in tunnels. International Journal of Rock Mechanics and Mining Sciences 64, 84-89.

Wang, C., Friedman, M., Li, Z. 2022. Hydraulic permeability and ageing behaviour of Dublin Port Tunnel, in: Rahman, M.a.J., M. (Ed.), The 20th International Conference on Soil Mechanics and Geotechnical Engineering, Sydney, Australia, pp. 1019-1024.

Wang, C., Friedman, M., Li, Z. 2023. Monitoring and assessment of a cross-passage twin tunnel long-term performance using wireless sensor network. Canadian Geotechnical Journal 60, 1140-1160.

Wongsaroj, J., Soga, K., Mair, R.J. 2013. Tunnelling-induced consolidation settlements in London Clay. Géotechnique 63, 1103-1115.

Wongsaroj, J., Soga, K., Mairr, J. 2007. Modelling of long-term ground response to tunnelling under St James's Park, London. Géotechnique 57, 75-90.

Xiao, Z., Osborne, J.A., Perez-Duenas, E., Li, Z. 2023. 3D modelling of the long-term hydromechanical performance of ageing tunnel at CERN in the molasse region. Tunnelling and Underground Space Technology.

Xu, P., Wu, Y., Huang, L., Zhang, K. 2021. Study on the Progressive Deterioration of Tunnel Lining Structures in Cold Regions Experiencing Freeze–Thaw Cycles, Applied Sciences.

Ye, Z., Liu, H. 2021. Investigating the relationship between erosion-induced structural damage and lining displacement parameters in shield tunnelling. Computers and Geotechnics 133, 104041.

Yi, S.-T., Hyun, T.-Y., Kim, J.-K. 2011. The effects of hydraulic pressure and crack width on water permeability of penetration crack-induced concrete. Construction and Building Materials 25, 2576-2583.

Yokozeki, K., Watanabe, K., Sakata, N., Otsuki, N. 2004. Modeling of leaching from cementitious materials used in underground environment. Applied Clay Science 26, 293-308.

Yoo, C. 2016. Hydraulic deterioration of geosynthetic filter drainage system in tunnels – its impact on structural performance of tunnel linings. Geosynthetics International 23, 463-480.

Závacký, M., Chalmovský, J., Stefanak, J., Mica, L., Bílek, P. 2018. Modelling of tunnel lining degradation, The 5th International Conference on Road and Rail Infrastructure, Zadar, Croatia, pp. 1499-1505.

Zhang, D.M., Ma, L.X., Zhang, J., Hicher, P.Y., Juang, C.H. 2015. Ground and tunnel responses induced by partial leakage in saturated clay with anisotropic permeability. Engineering Geology 189, 104-115.

Zhang, W., Qiu, J., Zhao, C. 2024. Structural behavior degradation of corroded metro tunnel lining segment. Structure and Infrastructure Engineering 20, 529-545.